

## **Iceberg trajectory modeling and meltwater injection in the Southern Ocean**

Rupert M. Gladstone and Grant R. Bigg

School of Environmental Sciences, University of East Anglia, Norwich, England, UK

Keith W. Nicholls

British Antarctic Survey, Cambridge, England, UK

**Abstract.** This is the first large-scale modeling study of iceberg trajectories and melt rates in the Southern Ocean. An iceberg model was seeded with climatological iceberg calving rates based on a calculation of the net surface accumulation from each snow catchment area on the Antarctic continent. In most areas, modeled trajectories show good agreement with observed patterns of iceberg motion, though discrepancies in the Weddell Sea have highlighted problems in the ocean general circulation model output used to force the iceberg model. The Coriolis force is found to be important in keeping bergs entrained in the coastal current around Antarctica, and topographic features are important in causing bergs to depart from the coastal regions. The modeled geographic distribution of iceberg meltwater joining the ocean has been calculated and is found in many near-coastal regions to be comparable in magnitude to the excess of precipitation over evaporation (P-E).

### **1. Introduction**

In recent years, iceberg models have been developed that predict drift tracks and melt rates of icebergs from the time of calving until erosion is complete, on an ocean-wide scale [Bigg *et. al.*, 1978; Matsumoto, 1996]. These models are forced by gridded data sets, typically output from circulation models, and have so far concentrated on the Arctic and North Atlantic Oceans. In developing such models, theory from earlier modeling studies of individual bergs [Loiset, 1993] or shorter time scales [Smith, 1993; Smith and Donaldson, 1987] has been used. Work stemming from investigations into the possibility of utilization of icebergs as a freshwater source [Weeks and Mellor, 1978] has also been of value.

The current study uses the model presented by Bigg *et. al.* [1997] with the following modifications: additional horizontal air and water drag forces on the top and bottom of icebergs, a periodic wind forcing term representing the passage of mesoscale weather systems, the introduction of a temperature dependence into the wave erosion term, damping of surface waves by sea ice, and the immobilization of icebergs that collide with the coast until changes in the forcing fields move them away.

The model was seeded with climatological iceberg calving fluxes (described in section 3) and validated in the Southern Ocean using published satellite observa-

tions. The aims are to reproduce and study the major features of Antarctic iceberg motion (section 4) and to predict the geographic distribution of iceberg meltwater injected into the Southern Ocean (section 5). This is the first large-scale modeling study of icebergs in the Southern Ocean.

The many potential applications for iceberg modeling include validation of ocean models, identification of shipping hazards, and the possible utilization of icebergs as a freshwater source. The main motivation for the present study is to identify regions of high meltwater injection into the oceans. This will be of particular use in ocean modeling, since prior to this study very little was known about where precipitation falling over the Antarctic Ice Sheet joins the Southern Ocean. Plans for future use of the model include the coupling of the model results with satellite imagery to make an assessment of the iceberg calving flux from Antarctica.

### **2. Iceberg Model**

The iceberg model is that of Bigg *et. al.* [1997]. The model summary given here (which includes some modifications) complements the full model description given by Bigg *et. al.* [1997]

The following climatological fields are used to force the model: European Centre for Medium-Range Weather Forecasts (ECMWF) reanalysis surface winds (monthly mean, resolution of 1.125° [Siefriid and Barnier, 1993]) and OCCAM ocean temperatures and ocean currents (top seven level average used, approximate depth 180 m, seasonal means from years 8 to 12 of climatological

Copyright 2001 by the American Geophysical Union.

Paper number 2000JC000347.  
0148-0227/01/2000JC000347\$09.00

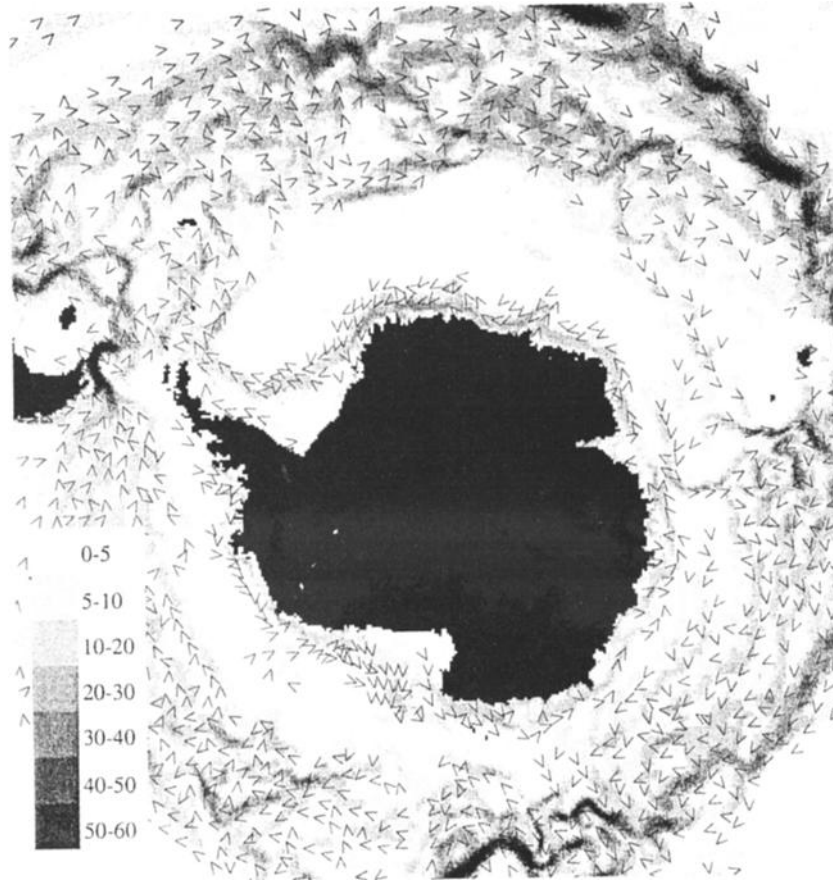


**Figure 1a.** Forcing fields used by the iceberg model (the April fields), showing ocean currents ( $\text{cm s}^{-1}$ ), average of upper  $\sim 180\text{m}$ . Arrowheads indicate direction of flow where  $> 5 \text{ cm s}^{-1}$ . See Figure 5 for longitude/latitude.

model run at 15-day intervals). The OCCAM land masking fields were also used for consistency (see Figures 1a, 1b, and 1c). OCCAM is an ocean general circulation model, run using ECMWF winds [*de Cuevas et al.*, 1999]. All OCCAM fields have a resolution of  $0.25^\circ$ . Monthly average sea-ice concentrations were taken from Scanning multichannel microwave radiometer (SMMR) and Special Sensor Microwave/Imager (SSM/I) satellite observations [*Schweitzer* [1995],  $2^\circ$  resolution], over the period 1973 to 1991. The forcing fields are gridded data sets. To determine the forcing for each iceberg, the bergs are assumed to occupy single points in space. Linear interpolation is used between the surrounding four grid points of the forcing fields.

A strong current flowing in a counterclockwise direction near to the Antarctic coast can be seen in the OCCAM ocean current fields (see Figure 1aa). This is henceforth referred to as the coastal current, though in regions where the continental shelf extends beyond the ice front, we often see this separate into a shelf break current and an ice front current, both within the east wind drift.

The ice fronts in OCCAM are modeled as vertical walls, hence effects due to circulation beneath the ice

shelves (which would tend to strengthen the coastal current [*Hellmer and Beckmann*, 1998]) are not included. This absence may be partially countered by the increased transfer of momentum from the wind directly to the ocean owing to the omission of sea ice from OCCAM.

The equation that describes the horizontal motion of an iceberg of mass  $M$  moving with velocity  $\mathbf{V}_i$  is

$$M \frac{d\mathbf{V}_i}{dt} = -Mf \times \mathbf{V}_i + \mathbf{F}_p + \mathbf{F}_w + \mathbf{F}_r + \mathbf{F}_a + \mathbf{F}_s, \quad (1)$$

where  $f$  is the Coriolis parameter;  $\mathbf{F}_p$  is the pressure gradient force exerted on the berg by the surrounding water;  $\mathbf{F}_r$  is the wave radiation force; and  $\mathbf{F}_a$ ,  $\mathbf{F}_w$ , and  $\mathbf{F}_s$  are the air form drag, water drag, and sea-ice drag, respectively. In this study,  $\mathbf{F}_a$  and  $\mathbf{F}_w$  have been modified to incorporate the effect of the stressing medium on the horizontal faces of the berg as well as the vertical. In this way, bergs with a greater ratio of horizontal to vertical extent are more realistically modeled. The drag coefficients used are taken from sea-ice models: 0.0012 for water on ice and 0.0055 for air on ice [*Mcphee*, 1980].

As in the work by *Bigg et al.* [1997], sea-ice drag is

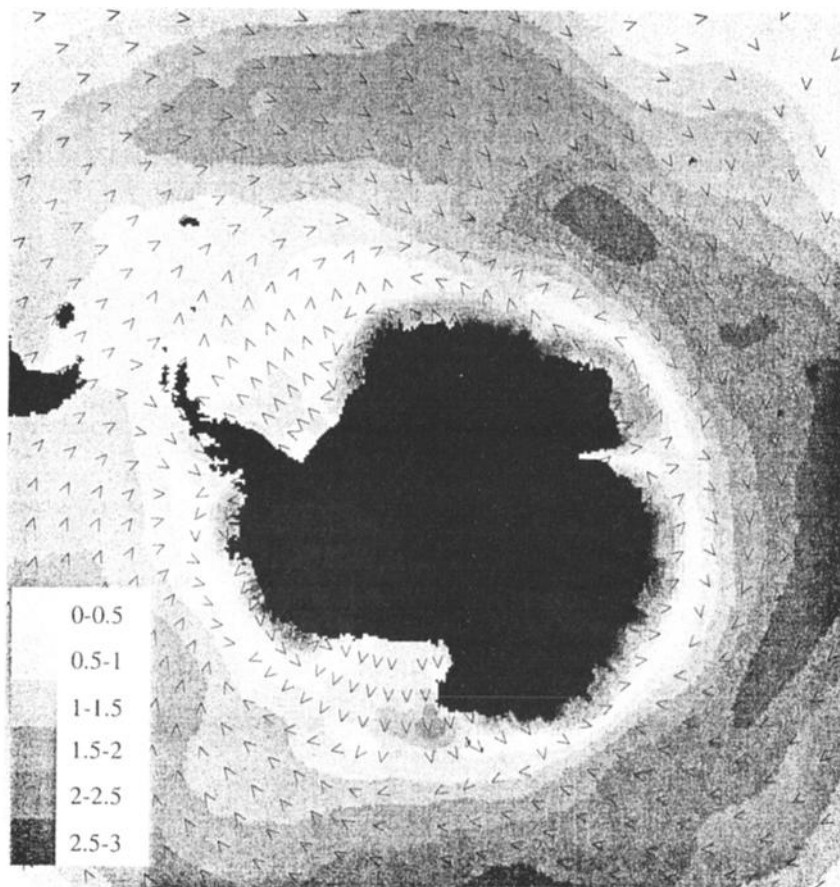


**Figure 1b.** Same as Figure 1a, but for wind stress ( $\text{N m}^{-2}$ ). Arrowheads indicate direction. See Figure 5 for longitude/latitude.

given the same drag coefficient as water and assumed to move with ocean currents. In the present study, for the purpose of calculating sea-ice drag, sea ice is given a thickness of 0 to 1 m in proportion to the sea-ice concentration. Although the three approximations outlined above probably underestimate the sea-ice drag, this component of the force budget is nearly always  $> 2$  orders of magnitude smaller than wind and ocean current drag. Errors in sea-ice drag are likely to be relevant only in extreme cases such as the presence of very thick fast ice along ice fronts or unusually thick, multiyear pack ice.

The pressure gradient force is calculated as by *Bigg et al.* [1997], using a rearrangement of the equation of motion for  $\mathbf{V}_w$ , the velocity of the water. In terms of forces per unit mass,  $\mathbf{V}_w$  is given by

$$\frac{d\mathbf{V}_w}{dt} + f \times \mathbf{V}_w = -\frac{1}{\rho_w} \nabla P + \frac{1}{\rho_w} \frac{\partial \tau}{\partial z}, \quad (2)$$

where  $P$  is the horizontal pressure field,  $\tau$  is the surface wind stress, and  $z$  is the vertical coordinate. In the present study the Coriolis term,  $f \times \mathbf{V}_w$ , is found to provide by far the largest contribution in the calculation of the pressure gradient force from (2). This results from approximate geostrophy in the ocean. Hence the

net force exerted on an iceberg by the pressure gradient force and the Coriolis force (the first two terms on the right-hand side of (1)) can be approximated by  $-Mf \times \mathbf{V}_r$ , where  $\mathbf{V}_r = \mathbf{V}_i - \mathbf{V}_w$ . This term arises from the deviation of the iceberg's motion from the geostrophic motion of the surrounding water, caused mainly by wind-related forcing ( $\mathbf{F}_a$  and  $\mathbf{F}_r$ ) and is referred to hereafter as "Coriolis-related forcing".

An extra  $10 \text{ m s}^{-1}$  has been added to the wind velocity in a  $2\frac{1}{2}$  day cycle: 12 hours eastward, 12 hours northward, 12 hours westward, 12 hours southward and 12 hours absent. This extra wind forcing has a magnitude and timescale similar to the wind associated with the passage of mesoscale weather systems [*King and Turner, 1997*]. This forcing is intended mainly to show the importance of short-timescale wind effects in iceberg modeling rather than as an accurate representation of storms. Note that by changing the wind forcing in this way, we introduce a small inconsistency between the winds and the ocean currents (since OCCAM, which provides our currents, did not use our extra wind forcing).

The main erosional terms in the model are wave erosion at the water level (which incorporates the calving of overhanging slabs) and turbulent heat transfer below

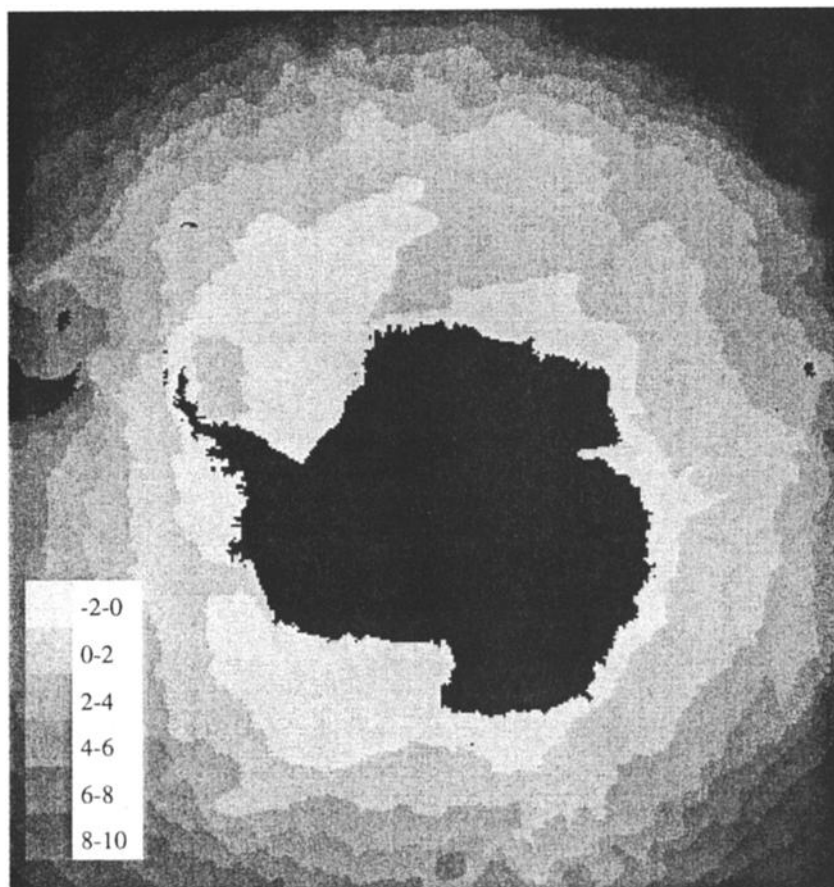


**Figure 1c.** Same as Figure 1a, but for surface temperature ( $^{\circ}\text{C}$ ). See Figure 5 for longitude/latitude.

the water level. Other terms include solar radiation and sensible heating above the water level and buoyant convection below the water level along the berg's sides.

Previous studies [*El-Tahan et al.*, 1987; *White et al.*, 1980] suggest that wave erosion increases approximately linearly with sea surface temperature. The wave erosion rate  $M_e$ , modified to incorporate temperature dependence, is now given (in  $\text{m d}^{-1}$ ) by

$$M_e = \frac{1}{6}(T + 2)S_s, \quad (3)$$

where  $S_s$  is the sea state (derived from the wind speed as by *Bigg et al.* [1997]) and  $T$  is the sea surface temperature.

Icebergs are assumed to remain tabular and maintain a constant length to width ratio (observations suggest that this is a reasonable assumption, see *Bigg et al.* [1997]). Erosional losses are incorporated in the model by reducing the length and/or thickness of the berg.

The way in which sea ice damps down surface waves has been incorporated by scaling the wave erosion term by  $\frac{1}{2}[1 + \cos(C^3\pi)]$ , where  $C$  is the sea-ice concentration. This function has been constructed such that its rate of decrease with respect to sea-ice concentration reaches a maximum at around 8/10 cover (in keeping with personal observations in the Weddell Sea, 1999). The effect

of this is to increase the lifetime of bergs in regions of high sea-ice concentrations and to shift modeled iceberg limits slightly equatorward.

Modeled icebergs are allowed to roll over. The Weeks-Mellor stability criterion is used [*Weeks and Mellor*, 1978]. Modeled bergs entering water shallower than the bergs' depth become grounded and remain stationary until they have melted sufficiently for them to drift off. Postcalving breakup of icebergs is not modeled. Icebergs that collide with the coast are held stationary until the forcing has changed sufficiently to push them away again.

### 3. Climatological Iceberg Calving

Iceberg calving fluxes and size distributions are needed in order to seed the iceberg model. The estimated calving fluxes are based on a calculation of balance fluxes using recent elevation [*Bamber and Bindshadler*, 1997] and net surface balance [*Vaughan et al.*, 1999] data sets. Balance fluxes are the fluxes of ice away from the ice sheet based on knowledge of the net snow accumulation rate at the ice sheet's surface and the assumption that the ice sheet is in steady state. The Antarctic grounding line has been divided into 29 sections, each of which has one corresponding iceberg release point, us-

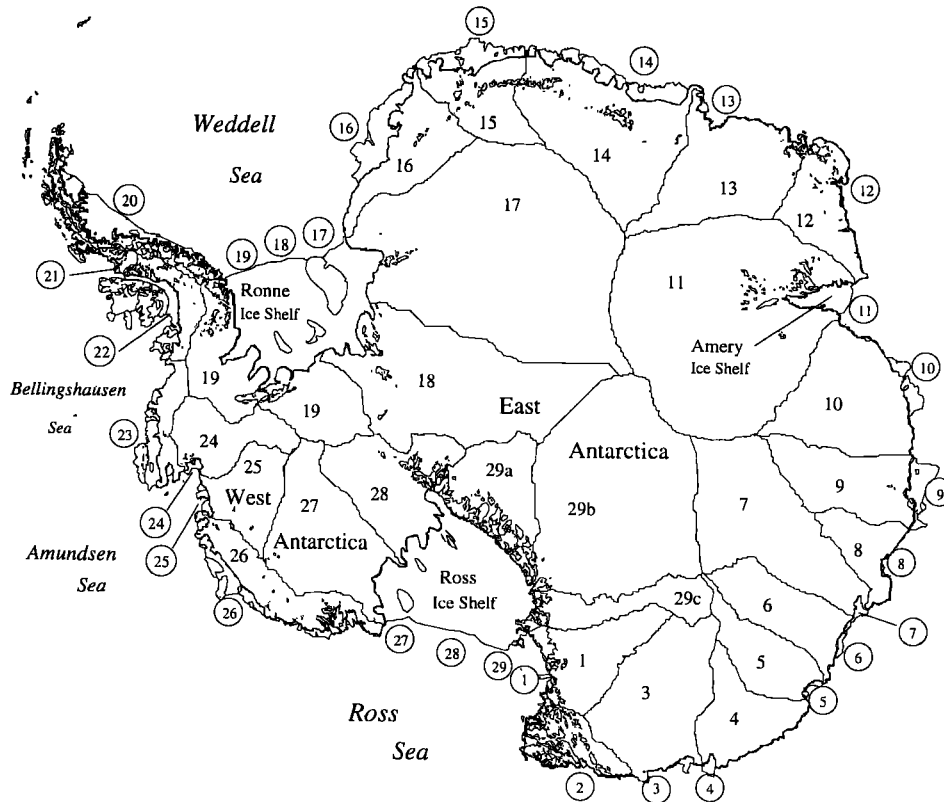


**Figure 2.** Catchment areas and calving sites. Bold line is the grounding line, and the thin lines inside it delineate catchment areas. The release sites, numbered from 1 to 29, correspond to those in Table 1. See Figure 5 for longitude/latitude.

ing the balance flux calculations of *Budd and Warner* [1996] as a guide. Using the techniques described by *Vaughan et al.*, [1999] (which are based on the assumption that the direction of ice flow is parallel to the surface slope), a geographical information system (GIS) was used to calculate the catchment area for each section of grounding line, and the net surface accumulation rate was integrated over each catchment area to provide balance fluxes across the grounding line. In extending these catchment areas from grounding line to ice front, flow lines were used as a guide (either modeled or observed *Jenkins et al.*, [1994]; *Thomas et al.*, [1984]) rather than GIS techniques. This is because factors other than surface slope are important in governing the direction of flow in ice shelves. In extending balance fluxes to the ice front, sparsely observed estimates of basal melt rates (e.g., *Jacobs et al.*, [1992]; *Jenkins and Doake*, [1991]; *Potter and Paren*, [1985]; *Thomas and MacAyeal*, [1982]) have been incorporated. Figure 2 shows the 29 release points and catchment areas.

Observations of cross grounding line or ice front fluxes were found in the literature [*Thomas et al.*, 1984; *Jenkins et al.*, 1997; *Frezzotti*, 1997] for regions corresponding to five of the catchments (regions 1, 2, 24, 27, and 28). The balance fluxes calculated here are higher than observed fluxes by between 10% and 30% in all five regions. This may be a result of increased snowfall over

the Antarctic Ice Sheet in recent decades [*Cullather et al.*, 1998, *Morgan et al.*, 1991]. Accordingly, the balance fluxes have been scaled down everywhere by 20% (except for the regions where observations were available, in which case the observed fluxes have been used) to provide an estimate of climatological calving fluxes. These fluxes are shown in Table 1. The numbers in the table correspond to the release site numbers in Figure 2. The total calving flux calculated here,  $1332 \text{ Gt yr}^{-1}$ , is near the lower end of the range of previously reported values (typically around  $2000 \text{ Gt yr}^{-1}$  [*Intergovernmental Panel on Climate Change (IPCC)*, 1995]). This is largely due to recent increases in basal melt rate estimates [*Jacobs et al.*, 1996]. In the current study the total basal melt rate for all Antarctic ice shelves is estimated at  $726 \text{ Gt yr}^{-1}$ . The negative ice front balance flux for section 26 (Table 1) is a result of a rather high estimate for basal melting. As this is an unrealistic situation, the calving flux in the model has been set to zero for section 26.

A size distribution containing 10 size classes of berg with maximum horizontal dimensions ranging from 60 to 2200 m has been chosen for all release points (see Table 2). The distribution is consistent with observations of Antarctic icebergs, which suggest that spatial variation of iceberg size distributions is not great near to the Antarctic coastline [*Wadhams*, 1988; *Orheim*, 1980;

**Table 1.** Climatological Calving Fluxes Based on the Balance Flux Calculations\*

Section	Ice Front Balance Flux (Gt yr <sup>-1</sup> )	Climatological Calving Flux (Gt yr <sup>-1</sup> )
1	25.4	20.3
2	29.8	23.8
3	70.7	56.6
4	67.8	54.3
5	52.8	42.4
6	55.7	44.8
7	78.2	62.6
8	59.2	47.4
9	109.9	91.3
10	73.5	60.3
11	72.7	54.3
12	41.5	33.2
13	64.0	51.3
14	76.8	61.4
15	41.9	33.5
16	48.3	38.6
17	74.5	55.9
18	27.4	13.5
19	140.4	114.6
20	80.6	69.8
21	75.7	62.1
22	29.0	17.5
23	21.9	10.4
24	28.4	28.4
25	57.7	43.7
26	-16.9	0.0
27	56.8	49.1
28	25.2	20.2
29	90.8	70.9

\*Balance fluxes across the ice front and climatological calving fluxes were used to seed the model (these are either observed fluxes or scaled down balance fluxes; see text).

*Budd et al.*, 1980]. Iceberg thickness has an upper limit for each release point given by the approximate thickness near the front of the ice shelf from which it calved, typically around 250 m.

The model has been run with calving spread evenly over four release dates: January, April, July, and Oc-

tober. A total of 1160 icebergs were modeled (10 size classes, 4 release dates, and 29 release points). The meltwater fluxes from the modeled bergs were scaled up using the calculated calving fluxes (as in Table 1) and weighted by the distribution column in Table 2 to generate the meltwater injection map (section 5). Note that this approach ignores the existence of giant bergs, the effects of which are discussed in section 4.1.

#### 4. Behavior of Modeled Icebergs in the Southern Ocean

The Antarctic iceberg model reproduced the three main modes of Antarctic iceberg motion inferred from observations by *Orheim* [1980]: westward drift in the coastal current, localized northward movement starting from within or near the coastal current, and eastward movement in and near the Antarctic Circumpolar Current (ACC).

Trajectories produced by the model are shown in Figure 3, which shows a high degree of entrainment of icebergs within the coastal current around almost the entire Antarctic coastline, except along the west coast of the Antarctic Peninsula and the Ronne-Filchner and Ross ice fronts. The west coast of the Antarctic Peninsula is poorly modeled with the resolution used here (1/4°). The high level of detail in the coastline, combined with the large number of calving sites with small calving fluxes, mean that much higher-resolution forcing and masking fields and a greater density of release points are required for a realistic study of iceberg movement and decay patterns in this area. Although some coastal drift of icebergs occurs along the Ross and Ronne-Filchner ice fronts, most iceberg trajectories have a strong northward component in these regions. This results from the absence of a coastal current in the OCCAM model along the major ice fronts (Figure 1a).

Movement of icebergs away from the coast is most intense in the following regions: near the tip of the Antarctic Peninsula (~55°W); over the Kerguelen Plateau (~85°E); in the Ross Sea (~180°E) and in the

**Table 2.** Iceberg Size Distribution\*

Size Class	Berg Thickness, m	Width, m	Length, m	Mass, kg	Distribution
1	40	40	60	$8.8 \times 10^7$	0.25
2	67	67	100	$4.1 \times 10^8$	0.12
3	133	133	200	$3.3 \times 10^9$	0.15
4	175	175	350	$1.8 \times 10^{10}$	0.18
5	250	333	500	$3.8 \times 10^{10}$	0.12
6	250	467	700	$7.5 \times 10^{10}$	0.07
7	250	600	900	$1.2 \times 10^{11}$	0.03
8	250	800	1200	$2.2 \times 10^{11}$	0.03
9	250	1067	1600	$3.9 \times 10^{11}$	0.03
10	250	1467	2200	$7.4 \times 10^{11}$	0.02

\*Berg thickness and mass are given for a calving thickness of 250 m. Calving thickness varies between 150 and 550 m depending on the thickness of the shelf from which the bergs calved.

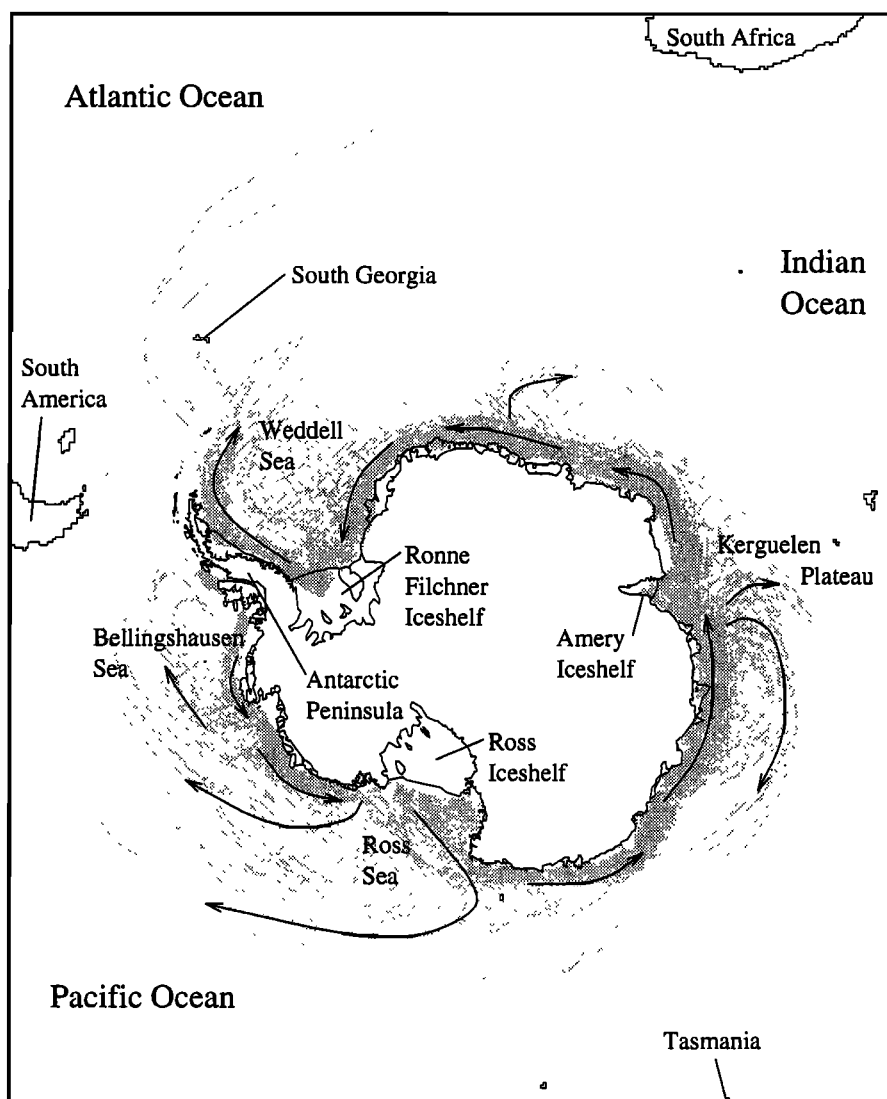


**Figure 3.** Modeled iceberg trajectories in the Southern Ocean (shaded area). Arrows indicate direction. See Figure 5 for longitude/latitude.

Bellingshausen Sea ( $\sim 100^\circ\text{W}$ ). The main cause of these regions of northward movement is topographic steering affecting ocean currents. This can be seen most clearly over the Kerguelen Plateau (see Figures 1a-1c and 4). Figure 4 also shows how crucial the berg's position within the coastal current is to whether an iceberg moves north or continues in the coastal current. A latitude change of just  $1^\circ$  or  $2^\circ$  can completely change an iceberg's trajectory. Icebergs only occasionally leave the coastal current away from these three regions.

When icebergs move northward into the west wind drift, subsequent motion is broadly similar in direction to that of the wind and currents, though given the highly filamented structure of ocean currents, paths of individual bergs can vary quite significantly.

Icebergs released in different seasons show differing patterns individually, but no clear seasonal movement trends are evident in bergs from different release sites.

This suggests that seasonal trends that may exist in iceberg calving would not have a large effect on the resulting iceberg movement patterns and meltwater distribution.

#### 4.1. Model Validation

*Tchernia and Jeannin*, [1984] used iceberg drift tracks from satellite tracking [*Tchernia and Jeannin*, 1983; *Vinje*, 1980] to examine the main trends in Antarctic iceberg motion (Figure 5). Modeled trajectories are similar to these movement patterns except for in the Weddell Sea, where observations suggest significant detrainment from the coastal current should occur around  $30^\circ\text{W}$ . The only modeled icebergs that leave the coast here are too small to drift far. Four icebergs tracked from near the Ronne Ice Front in 1999 moved northwestward to around  $75^\circ\text{S}$  and then generally northward parallel to the east coast of the Antarctic peninsula,

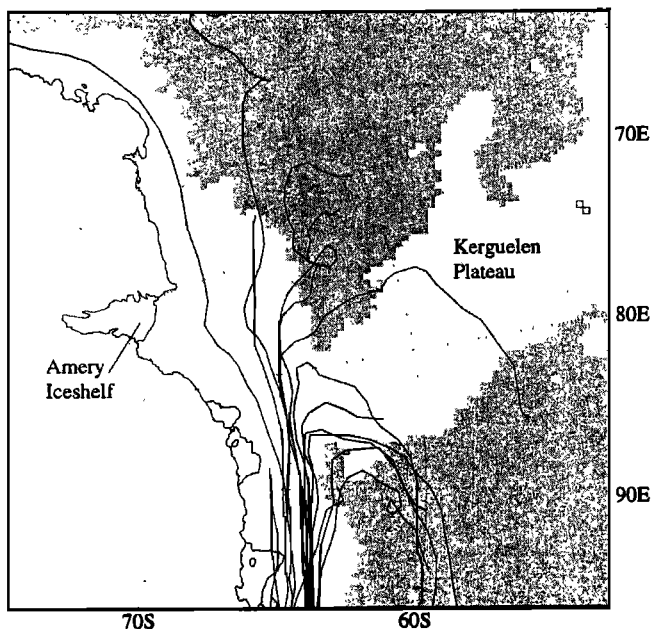


**Figure 4.** Modeled iceberg drift tracks from release site 6 (see Figure 2) in the region of the Kerguelen Plateau. Light gray represents an ocean depth  $> 1000$  m, and dark gray a depth of  $> 3700$  m.

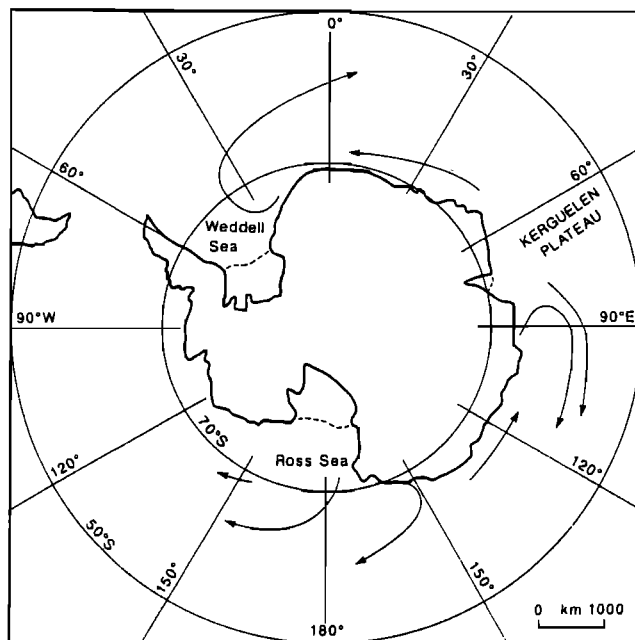


**Figure 5.** Main trend of movement shown by satellite-tracked icebergs in the Southern Ocean (reprinted, with permission from Cambridge University Press, from *Tchernia and Jeannin* [1984]).

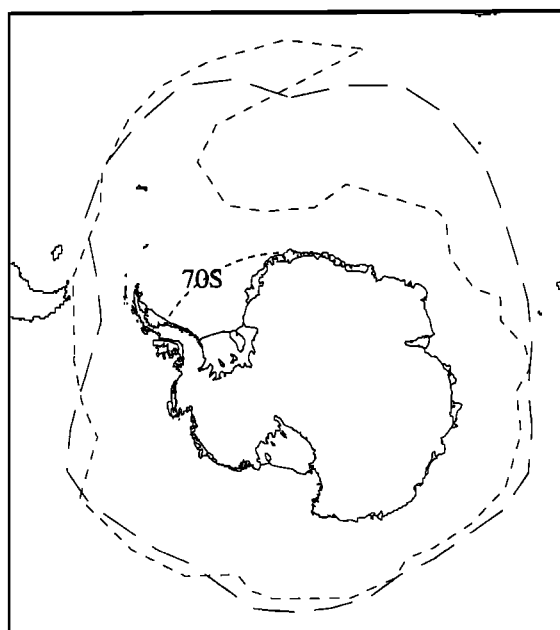
exhibiting motion similar to modeled iceberg motion. These bergs were still under observation at the time of writing (E. Fahrbach, personal communication, 1999). Modelled trajectories in the Ross Sea are similar to trajectories reported by *Keys and Fowler* [1989].

Figure 6 shows a comparison of modeled and observed iceberg limits. Again, agreement is good in all regions except the Weddell Sea, where modeled icebergs move too far north and not far enough east. Since the model works well in other regions around Antarctica, it seems likely that it is the forcing that is problematic.

A model run with icebergs being released at  $70^{\circ}\text{S}$  (representing bergs escaping from the coastal current at around  $30^{\circ}\text{W}$ ) in the Weddell Sea shows much better agreement with observations, in terms of both limits and trajectories. This suggests that problems with modeled icebergs in the Weddell Sea would be much reduced if the forcing were such that more of the large bergs (size classes 6-10) left the coast at around  $30^{\circ}\text{W}$ . The errors in the forcing are probably therefore only in the southern Weddell Sea. It may be that the ECMWF winds or the OCCAM currents are not good in this area or that it is an area of particularly high mesocyclonic activity. OCCAM has several deficiencies in this region: subice shelf circulation is not included, sea ice is not included, and the ice front is not mapped correctly. Any of these could affect upper ocean currents and hence iceberg motion.

One of the important differences between Northern Hemisphere and Southern Hemisphere icebergs is the existence in the Southern Ocean of "giant" icebergs, defined for the purposes of satellite tracking as greater than 10 nautical miles (18.52 km) in horizontal extent.

Some of the large Antarctic ice shelves tend to calve occasional giant bergs instead of frequently calving regular size bergs. Giant icebergs are thought to account for as much as 50% [*Jacobs et al.*, 1992] of the total Antarctic iceberg calving flux, though they are not



**Figure 6.** Observed northernmost iceberg limits (from *Soviet Antarctic Survey* [1966], long-dashed line) and modeled iceberg limits (dash-dotted line). The dotted line shows modeled limits when icebergs are released at  $70^{\circ}\text{S}$  (short-dashed line) in the Weddell Sea. See Figure 5 for longitude/latitude.

included in the present iceberg model. The planned development of the model to include giant bergs may be problematic: the current method is to treat each berg as a single point and to calculate the forcing fields at the berg's location. This is a poor approximation for bergs whose horizontal extent is greater than the width of ocean currents [Keys *et. al.*, 1990]. It would also be necessary to model the postcalving breakup of giant bergs.

#### 4.2. Modeled Iceberg Dynamics

The largest forces a regular sized iceberg (horizontal extent of  $10^2$  to  $10^3$  m) is subjected to are the water and air drag forces. These are of similar magnitude and importance to iceberg dynamics. The wave radiation force and Coriolis-related forces are typically up to an order of magnitude smaller, though the Coriolis-related forces are still important (explained below). The sea-ice drag is typically 2 orders of magnitude smaller.

The model results are not highly sensitive to changes in the various drag coefficients, nor to variations in the initial size distribution, within realistic limits. Results are quite sensitive to changes in the thermodynamic terms. This is largely a result of the currently limited knowledge and understanding of iceberg melting, which provide only a weak constraint on the model parameterizations. However, the agreement between modeled and observed limits suggests our melting term is a reasonable approximation.

Figure 7 illustrates the balance in the principal forces acting on a typical iceberg moving westward in the coastal current when the westward component of the wind causes the iceberg to move to the west faster than the surrounding water. Icebergs near the coast will be subjected to a mixture of the east wind drift and katabatic winds, which can reach to more than 100 km from the coast [King and Turner, 1997]. The Coriolis-related forcing approximates to  $-Mf \times \mathbf{V}_r$  and therefore acts at  $90^\circ$  to the left of  $\mathbf{V}_r$ . For a typical forcing regime

near to the Antarctic coast the Coriolis-related forcing therefore acts to the south and is important in preventing widespread detrainment of bergs from the coastal current. It is also more significant for larger bergs than for smaller ones. This is because the Coriolis-related forcing is proportional to the mass of the berg, which increases more rapidly with berg size than does surface area, to which the air and water drag forces are proportional. Since the latitudinal position of an iceberg within the coastal current is a crucial factor affecting detrainment, the Coriolis-related forcing has the important effect of encouraging larger bergs to stay entrained in the coastal current while smaller bergs may move northward. A model run with the Coriolis force and the pressure gradient force removed from equation (1) showed widespread northward motion around the whole Antarctic coastline with very little coastal drift, instead of the regional detrainment seen in Figure 3. In physical terms the wind forcing causes the iceberg to move at a different speed than the surrounding ocean currents (which are approximately geostrophic), hence the oceanic pressure gradient force no longer balances the Coriolis force exerted on the iceberg.

The mesoscale wind forcing induces small meanders in iceberg trajectories, causing a greater proportion of bergs to leave the coastal current compared with a control run that used just the climatological wind forcing. This increase in detrainment is not large. It is due to the sensitivity of detrainment to small latitudinal changes in position within the coastal current.

#### 5. Meltwater Injection

Figure 8 shows the meltwater production rates from the climatological model run. This iceberg melt is caused mainly by wave erosion (which includes calving of overhanging slabs) and by turbulent heat transfer from the surrounding water. Over most of the Southern Ocean, input of iceberg meltwater is small compared with the excess of precipitation over evaporation (P-E)

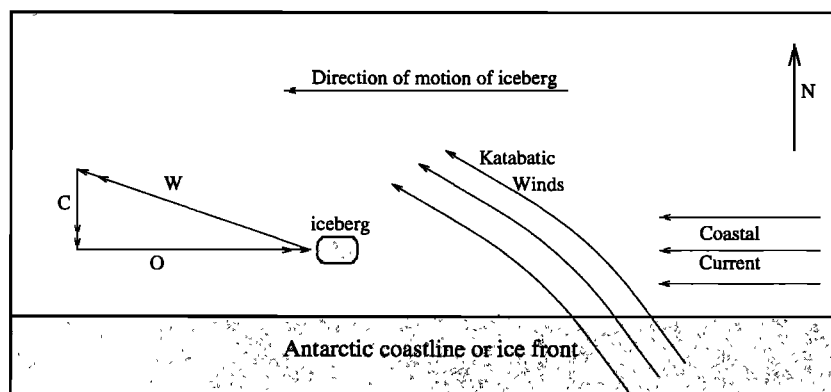


**Figure 7.** Schematic diagram showing the force balance for a typical iceberg moving westward in the coastal current. Typical wind and ocean current directions are indicated. The main forces are wind-related forcing (W) (includes wave radiation force), Coriolis-related forcing (C) (includes oceanic pressure gradient force), and ocean-current drag (O).

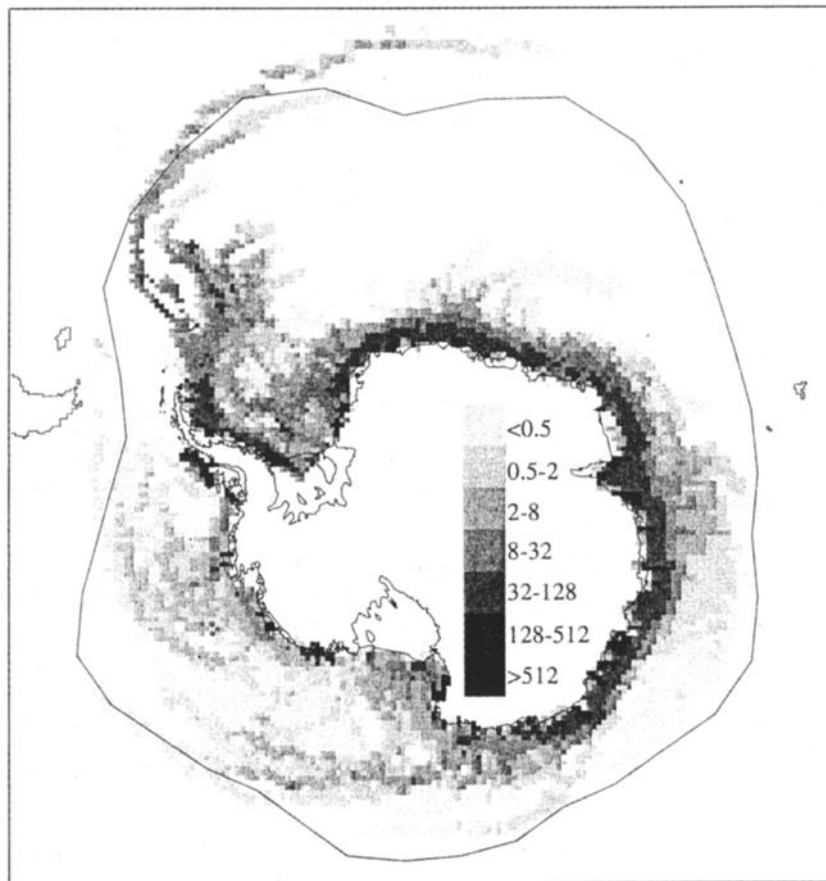


**Figure 8.** Spatial variation in modeled iceberg meltwater injected into the ocean (units are  $\text{mm yr}^{-1}$  rainfall equivalent). The northern limit of iceberg fields based on observations (as in Figure 6) is also shown. See Figure 5 for longitude/latitude.

[Turner *et. al.*, 1999]. The magnitudes are comparable, however, in areas close to much of the Antarctic coastline. The effects of the absence of giant bergs from the current study are not clear, since although giant bergs will last longer (and hence one might expect them to shift the distribution of meltwater northward), the arguments presented in section 4.2 suggest that they may also stay in the coastal drift for longer (and thus concentrate meltwater farther south).

There are important differences in the oceanographic impact between freshwater being added as a result of P-E and as a result of the melting of icebergs (and, indeed, ice shelves). In the case of P-E the majority of the latent heat to melt the snowfall comes from the atmosphere: the snow melts either in the surface layers of the ocean, which are warmed by the atmosphere, or in the atmosphere itself to generate rain. In the case of icebergs a large proportion of the latent heat comes from the ocean, at depths given by iceberg keel depths. Another difference is that the P-E input is strongly seasonal, as snowfall is captured by sea ice and released during the summer retreat.

### 5.1. Effects of Iceberg Melt

The impact of icebergs melting into the sea depends on the ambient hydrography and the iceberg draft. When seawater melts ice, the mixture of melt and ambient water lies on a straight line in temperature-salinity ( $T-S$ ) space, with a characteristic gradient of  $\sim 2.5^\circ\text{C psu}^{-1}$  [Gade, 1979]. Jenkins [1999] shows that if the gradient of the ambient  $T-S$  characteristic is higher than that of the meltwater mixture gradient, an upwelling mixture will be warmer than its surroundings. If the ambient  $T-S$  gradient is below the meltwater mixture gradient, the upwelling mixture will be cooler than the ambient water, possibly resulting in the production of water at depth with a temperature below the surface freezing point.

For most of the Southern Ocean the  $T-S$  characteristic through the thermocline has a gradient greater than  $2.5^\circ\text{C psu}^{-1}$  [Jenkins, 1999]. The basal melting of an iceberg thick enough to reach down into the thermocline therefore causes upwelling of relatively warm and saline water.

Jenkins [1999] estimates a vertical heat flux local to

icebergs in the Southern Ocean of between 150 and 300  $W m^{-2}$ . The effect of upwelling on the stability of the water column depends on whether it produces interleaving warm salty layers (no effect on stability) or whether the upwelling mixture is buoyant enough to ascend all the way to the surface. In the latter case the result will generally be an increase in the water column stability. Few observations have been made in the vicinity of icebergs, but an idea of the effects can be obtained by regarding ice shelves as tethered icebergs. The waters at the northern ice front of George VI Ice Shelf provide an example of an upwelling circumpolar deep water (CDW)/meltwater mixture that sits at the top of the water column, giving a net increase in stability [Potter *et al.*, 1988]. The vertical heat flux associated with the upwelled water will have the additional effect of reducing sea-ice formation rates, again contributing to the water column stability. The water column in the vicinity of Pine Island Glacier is an example of CDW/meltwater mixtures that appear as intrusions. The intrusions do not affect the stability directly but, again, provide heat to the surface layers that is likely to reduce sea-ice formation rates [Hellmer *et al.*, 1998].

Icebergs that are not thick enough to penetrate the thermocline cool and freshen the upper layers when they melt, helping stabilize the water column. Similarly, melting of sidewalls and calved fragments will generally enhance water column stability.

Melting of icebergs over the continental shelf can have consequences for processes at the shelf break. Hellmer and Beckmann [1998] used a modeling study to show that disabling the melt from ice shelves in the Weddell Sea has the effect of reducing the strength of the Antarctic shelf break current. This is a consequence of the reduced salinity gradient across the oceanographic front at the shelf break. The effect is to decrease the transport of heat and salt into the southern Weddell Sea. Converse arguments suggest that the effect of icebergs melting over the continental shelves is to strengthen the shelf break current and therefore increase the transport of heat and salt along the southern limits of the Weddell Gyre. In the Bellingshausen and Amundsen Seas, warmer off-shelf waters have free access to the continental shelf and there is no significant shelf break front or current.

## 5.2. Implications for This Study

Melting of icebergs over the continental shelf will tend to augment the effect of ice shelves in the region. For example, the model predicts a band of high meltwater fluxes over the broad continental shelf of the east coast of the Antarctic Peninsula. As cold shelf waters dominate this region, the effect will be to help freshen and cool the water column, possibly to temperatures below the surface freezing point by analogy with the effect of ice shelves in the region. Water that is "potentially supercooled" in this way is defined as ice shelf water

(ISW). Production of ISW from icebergs would add to the ISW production beneath the ice shelves along the coast. The coastal current will also be enhanced as a result of the freshening on the continental shelf.

It is tempting to speculate that the pattern of iceberg melt over the deep ocean helps to select regions prone to deep convection. For example, Figure 8 indicates that the area covered by the Weddell Polynya during the mid-1970s is one of the few regions close to the continent that has relatively little freshwater added by iceberg melt. Such ideas can only be tested when we have a fuller understanding of the impact of icebergs on the ocean waters in which they float.

Icebergs clearly have several competing effects on the local water column, some of which have been outlined above. Without an analysis of each effect, which is beyond the scope of this study, it is not possible to be confident of the net result.

## 6. Conclusions

The iceberg model has been shown to reproduce iceberg movement and limits consistent with observations in most areas of the Southern Ocean (except the southern Weddell Sea and near the west coast of the Antarctic Peninsula). Examination of the regions where it is less successful has highlighted shortcomings in the OC-CAM general circulation model. The use of an ocean model without these shortcomings would be expected to improve the trajectories given by the iceberg model for these regions.

The greater quantity of observed, long-term iceberg drift tracks available for the Southern Ocean ( $\sim 40$  were used to validate the iceberg model in the present study) has enabled a more rigorous testing of the model than was possible for the Arctic and North Atlantic Oceans. The resulting corrections and modifications will benefit future modeling studies in both the Southern and Northern Hemispheres.

Understanding of some aspects of iceberg dynamics has been increased through this modeling study, in particular, the effects of Coriolis-related forcing on an iceberg in the presence of winds. For most regions of the Southern Ocean the model has offered a more detailed picture of typical iceberg movement patterns than can be determined from the limited number of observed iceberg drift tracks.

Section 5 demonstrated how the iceberg model can be used to predict the geographic distribution of iceberg meltwater injection. The resulting meltwater injection density map (Figure 8), while not being truly representative owing to the omission of giant bergs, suggests that there exist regions where meltwater injection is at least as significant to the freshwater balance as P-E.

### Acknowledgments.

Thanks are owed to David Vaughan for advice with the balance flux calculations and to Jonathon Bamber, David

Vaughan, Beverly de Cuevas, and Eberhard Fahrback for making various data sets available for this project. We also wish to thank the reviewers for their suggestions. This paper forms part of the Ph.D. work of Rupert Gladstone, funded by NERC as a CASE student with BAS.

## References

- Bamber, J. L., and R. A. Bindshadler, An improved elevation data set for climate and ice sheet modelling: Validation with satellite imagery, *Ann. Glaciol.*, **25**, 439-444, 1997.
- Bigg, G. R., M. R. Wadley, D. P. Stevens, and J. A. Johnson, Modelling the dynamics and thermodynamics of icebergs, *Cold Reg. Sci. Technol.*, **26**, 113-135, 1997.
- Budd, W. F., and R. C. Warner, A computer scheme for rapid calculations of balance-flux distributions, *Ann. Glaciol.*, **23**, 21-27, 1996.
- Budd, W.F., T. H. Jacka, and V. I. Morgan, Antarctic iceberg melt rates derived from size distributions and movement rates, *Ann. Glaciol.*, **1**, 103-112, 1980.
- Cullather, R. I., D. H. Bromwich, and M. L. Van Woert, Spatial and temporal variability of Antarctic precipitation from atmospheric methods, *J. Clim.*, **11**, 334-367, 1998.
- de Cuevas, B. A., D. J. Webb, A. C. Coward, C. S. Richmond, and E. Rourke, The UK ocean circulation and advanced modelling project (OCCAM), in *Proceedings of HPCI Conference 1998, Manchester 12-14 January, 1998*, edited by R.J. Allan, M.F. Guest, A.D. Simpson, D.S. Henty, and D.A. Nicole, *High Performance Comput.*, pp. 325-335, Plenum Press, 1999.
- El-Tahan, M. S., S. Venkatesh, and H. El-Tahan, Validation and quantitative assessment of the deterioration mechanisms of Arctic icebergs, *J. Offshore Mech. Arctic Eng.*, **109**, 102-108, 1987.
- Frezzotti, M., Ice front fluctuation, iceberg-calving flux and mass balance of Victoria land glaciers, *J. Phys. Oceanogr.*, **9**, 61-73, 1997.
- Gade, H. G., Melting of ice in sea water: A primitive model with application to the Antarctic ice shelf and icebergs, *J. Phys. Oceanogr.*, **9**, 189-198, 1979.
- Hellmer, H. H., and A. Beckmann, The influence of ice shelves on the Weddell Sea, *Filchner-Ronne Ice Shelf Programme Rep. 12*, Alfred-Wegener-Inst. for Polar and Mar. Res., Bremerhaven, Germany, 1998.
- Hellmer, H. H., S. S. Jacobs, and A. Jenkins, Oceanic erosion of a floating Antarctic glacier in the Amundsen Sea, in *Ocean, Ice, and Atmosphere: Interactions at the Antarctic Continental Margin*, edited by S. S. Jacobs and R. F. Weiss, *Antarct. Res. Ser.*, vol 75, pp. 83-100, AGU, Washington, D.C., 1998.
- Intergovernmental Panel on Climate Change. The Science of Climate Change, Cambridge Univ. Press, New York, 1995.
- Jacobs, S. S., H. H. Hellmer, C. S. M. Doake, A. Jenkins, and R. M. Frolich, Melting of ice shelves and the mass balance of Antarctica, *J. Glaciol.*, **38** (130), 375-387, 1992.
- Jacobs, S. S., H. H. Hellmer, and A. Jenkins, Antarctic ice sheet melting in the Southeast Pacific, *Geophys. Res. Lett.*, **23** (9), 957-960, 1996.
- Jenkins, A., The impact of melting ice on ocean waters, *J. Phys. Oceanogr.*, **29**, 2370-2381, 1999.
- Jenkins, A., and C. S. M. Doake, Ice ocean interaction on Ronne Ice Shelf, Antarctica, *J. Geophys. Res.*, **96** (C1), 791-813, 1991.
- Jenkins, A., D. G. Vaughan, and C. S. M. Doake, Numerical modelling of the Filchner-Ronne Ice Shelf, *Filchner-Ronne Ice Shelf Programme Rep. 8*, Alfred-Wegener-Inst. for Polar and Mar. Res., Bremerhaven, Germany, 1994.
- Jenkins, A., D. G. Vaughan, S. S. Jacobs, H. H. Hellmer, and J. R. Keys, Glaciological and oceanographic evidence of high melt rates beneath Pine Island Glacier, West Antarctica, *J. Glaciol.*, **43** (143), 114-121, 1997.
- Keys, H., and D. Fowler, Sources and movement of icebergs in the south-west Ross Sea, Antarctica, *Ann. Glaciol.*, **12**, 85-88, 1989.
- Keys, H. J. R., S. S. Jacobs., and D. Barnett, The calving and drift of iceberg B-9 in the Ross Sea, Antarctica, *Antarct. Sci.*, **2**, 243-257, 1990.
- King, J. C., and J. Turner, *Antarctic Meteorology and Climatology*, Cambridge Univ. Press, New York, 1997.
- Løset, S., Thermal energy conservation in icebergs and tracking by temperature, *J. Geophys. Res.*, **98**, (C6), 10,001-10,012, 1993.
- Matsumoto, K., An iceberg drift and decay model to compute the ice-rafted debris and iceberg meltwater flux: Application to the interglacial North Atlantic, *Paleoceanography*, **11** (6), 729-742, 1996.
- McPhee, M. G., An analysis of pack ice drift in summer, in *Sea Ice Processes and Models*, edited by R.S. Pritchard, pp. 62-75, University of Washington, Seattle, 1980.
- Morgan, V. I., I. D. Goodwin, D. M. Etheridge, and C. W. Wookey, Evidence from Antarctic ice cores for recent increases in snow accumulation, *Nature*, **354**, 58-60, 1991.
- Orheim, O., Physical characteristics and life expectancy of tabular Antarctic icebergs, *Ann. Glaciol.*, **1**, 11-18, 1980.
- Potter, J. R., and J. G. Paren, Interaction between ice shelf and ocean in George VI Sound, Antarctica, in *Oceanology of the Antarctic Continental Shelf*, *Antarct. Res. Ser.*, vol.43, edited by S.S. Jacobs, pp. 35-58, AGU, Washington, D.C., 1985.
- Potter, J. R., M. H. Talbot, and J. G. Paren, Oceanic regimes at the ice fronts of Goerge VI Sound, Antarctic Peninsula, *Cont. Shelf. Res.*, **8**, 347-362, 1988.
- Schweitzer, Monthly Average Sea-Ice Concentration, *Rep. DDS-27*, <http://geochange.er.usgs.gov/pub/info/holdings-s.html>, U. S. Geol. Surv., Reston, Virginia, 1995.
- Siefridt, L., and B. Barnier, Banque de Donnees AVISO Vent/flux: Climatologie des Analyses de Surface du CEP-MMT, *Rep. 91 1430 025*, 43 pp, Meteo-France, Toulouse, 1993.
- Smith, S. D., Hindcasting iceberg drift using current profiles and winds, *Cold Reg. Sci. Technol.*, **22**, 33-45, 1993.
- Smith, S. D., and N. R. Donaldson, Dynamic modelling of iceberg drift using current profiles, *Can. Tech. Rep. Hydrogr. Ocean Sci.*, **91**, 1987.
- Soviet Antarctic Survey, *Antarctic Atlas*, Moscow, 1966.
- Tchernia, P., and P. F. Jeannin, *Quelques Aspects de la Circulation Océanique Antarctique Révélés par l'observation de la Dérive d'icebergs (1972-1983)*, Lab. d'Océanogr. Phys. du Muséum Nat. d'Histoire Naturelle de Paris, Paris, 1983.
- Tchernia. P., and P. F. Jeannin, Circulation in Antarctic waters as revealed by iceberg tracks 1972-1983, *Polar Rec.*, **22** (138), 263-269, 1984.
- Thomas, R. H., and D. R. MacAyeal, Derived characteristics of the Ross Ice Shelf, Antarctica, *J. Glaciol.*, **28** (100), 397-412, 1982.
- Thomas, R. H., D. R. MacAyeal, D. H. Eilers, and D. R. Gaylord, Glaciological studies on the Ross Ice Shelf, Antarctica, 1973-1978, in *The Ross Ice Shelf: Glaciology and Geophysics*, vol. 42, edited by C. R. Bentley and D. E. Hayes, pp. 21-53, AGU, Washington, D. C., 1984.
- Turner, J., W. M. Connolley, S. Loenard, G. J. Marshall, and D. G. Vaughan, Spatial and temporal variability of net snow accumulation over the Antarctic from ECMWF re-analysis project data, *Int. J. Clim.*, **19**, 697-724, 1999.
- Vaughan, D. G., J. L. Bamber, M. Giovinetto, J. Russell,

- and P. R. Cooper, Reassessment of net surface balance in Antarctica, *J. Clim.*, 12, 933-946, 1999.
- Vinje, T. E., Some satellite-tracked iceberg drifts in the Antarctic, *Ann. Glaciol.*, 1, 83-87, 1980.
- Wadhams, P., Winter observations of iceberg frequencies and sizes in the South Atlantic Ocean, *J. Geophys. Res.*, 93, (C4), 3583-3590, 1988.
- Weeks, W. F., and M. Mellor, Some elements of iceberg technology, in *Proceedings of the first Conference on Iceberg Utilization for Freshwater Production*, edited by A.A. Hussein, pp. 45-98, Iowa State Univ., 1978.
- White, F. M., M. L. Spaulding and L. Gominho, Theoretical estimates of the various mechanisms involved in iceberg deterioration in the open ocean environment, Rep. CG-D-62-80, U.S. Coast Guard Res. and Dev. Cent., Rhode Island Univ., Kingston, 1980.
- 
- G. R. Bigg and R. M. Gladstone, School of Environmental Sciences, University of East Anglia, Norwich NR4 7TJ, England, UK.
- K.W. Nicholls, Ice and Climate Division, British Antarctic Survey, High Cross, Madingley Road, Cambridge CB3 0ET, England, UK.

(Received March 29, 2000; revised December 22, 2000; accepted February 12, 2001.)